Aerosol and Air Quality Research, 17: 59–68, 2017

ISSN: 1680-8584 print / 2071-1409 online
doi: 10.4209/aaqr.2016.01.0029

A Chamber Study of Secondary Organic Aerosol (SOA) Formed by Ozonolysis of *d*-Limonene in the Presence of NO

Fei Chen[1,2,3], Hao Zhou[3], Jixi Gao[1,2], Philip K. Hopke[3*]

[1] *Nanjing Institute of Environmental Sciences, Ministry of Environmental Protection, Nanjing 210042, China*
[2] *Jiangsu Collaborative Innovation Center of Atmospheric Environment and Equipment Technology (CICAEET), Nanjing University of Information Science Technology, Jiangsu 210044, China*
[3] *Center for Air Resource Engineering and Science, Clarkson University, Potsdam, New York 13699, USA*

ABSTRACT

Experiments were conducted in a dynamic chamber system to measure the formation of secondary organic aerosol (SOA) and particle-bound reactive oxygen species (ROS) produced from limonene ozonolysis in the presence of NO by varying the ratio of O_3 to NO. A diffusion cell system was used to produce the constant input of limonene in to the chamber, and six sets of experiments were conducted. The concentration of SOA mass and ROS produced were measured at steady-state. ROS, including peroxides, peroxy radicals and ions, was determined using dichlorofluorescin (DCFH) and converted to equivalent H_2O_2 concentration. The particle mass was measured using a tapered element oscillating microbalance (TEOM) and a scanning mobility particle sizer (SMPS) was used to obtain particle volume distributions. The results showed that the SOA mass concentration ranged from 30.3 to 157.3 μg m^{-3}, and the ROS concentration ranged from 6.1 to 29.4 nmol m^{-3} of H_2O_2. For the different combinations of NO_x and O_3, the concentration ratio of $[O_3]/[NO]$ around 1 was found to produce highest SOA mass and ROS, which is 157.3 μg m^{-3} and 29.4 nmol m^{-3}. The SOA density was estimated by comparing the mass concentrations with the volume concentrations ranged from 1.21 to 1.48 g cm^{-3}. The highest SOA density (1.48 g cm^{-3}) occurred with the lowest concentration ratio of $[O_3]/[NO]$. Compared with other monoterpene and linalool where each has one unsaturated carbon bond in other studies, limonene which has two unsaturated carbon bonds. Thus, it is the most efficient in generating the SOA and ROS concentrations in prior experiments without NO present.

Keywords: *d*-Limonene; Secondary organic aerosol; NO; Reactive oxygen species; Indoor air pollution.

INTRODUCTION

Indoor air pollution has attracted public attention for its effect on personal and public health, with substantial focus on emission, transport, formation and removal pathways (Guenther *et al.*, 2000). Many studies (Li *et al.*, 2002; Docherty *et al.*, 2005; Presto *et al.*, 2005; Zhang *et al.*, 2006) have suggested that reactions between the unsaturated terpenoids that originate from indoor sources such as consumer products (Singer *et al.*, 2006a, b) and ozone (O_3), which originates outdoors, may produce secondary organic aerosol (SOA) in the indoor atmosphere (Weschler and Shields, 1999; Weschler, 2004; 2006; Morawska *et al.*, 2009; Carslaw *et al.*, 2012). Indoor ozone can originate from indoor sources such as laser printers and other office equipment (Destaillats *et al.*, 2009) and by infiltration from the ambient environment (Weschler *et al.*, 1989; Weschler, 2000; Du and Liu, 2009). These reactions also yield a variety of reactive intermediates, such as hydroxyl radicals (OH), alkylperoxy radicals (RO_2), and Criegee intermediates (Wescher and Shields, 1996; Kamens *et al.*, 1999; Leungsakul *et al.*, 2005; Venkatachari and Hopke, 2008; Pavlovic and Hopke, 2010; Waring *et al.*, 2011). These oxidative species could lead to adverse health effects (Weschler, 2006).

Previous studies of indoor SOA formation have focused on single terpenes ozonolysis, such as α-pinene, limonene, and limonoketone (Hatfield and Hartz, 2011; Lee *et al.*, 2011; Santiago *et al.*, 2012; Youssefi and Waring, 2012). Limonene is a prevalent terpene with a strong orange-like fragrance found in a number of household consumer products used indoors. The National Library of Medicine's (NLM) Household Products Database (HHS/NIH, 2015) lists 166 consumer products that contain *d*-limonene as an ingredient. Also there can be substantial concentrations of NO_x in indoor air arising from combustion appliances such as gas stoves (Lee *et al.*, 2002) and increase of vehicle

* Corresponding author.
Tel.: +1 315 268 3861; Fax: +1 315 268 4410
E-mail address: phopke@clarkson.edu

population. However, limonene ozonolysis with nitric oxide (NO) present has received relatively little consideration even though NO_x would react with other peroxy radicals and change the SOA formation pathways. Nojgaard *et al.* (2006) studied the effect of the nitrogen dioxide (NO_2) concentration on particle formation of *d*-limonene ozonolysis, and has found the presence of NO_2 resulting in formation of the nitrate radical introduced an additional loss term for ozone. As a result, the observed decrease in particle concentration from *d*-limonene/O_3/NO_2 mixtures was ascribed to the O_3/NO_2 reaction.

Spittler *et al.* (2006) have studied the reactions of NO_3 radicals with limonene and α-pinene, including reaction products and SOA formation. In addition to a large yield of unidentified organic nitrates, pinonaldehyde and endolim have been identified as the major reaction products of the NO_3 radical initiated oxidation of α-pinene and limonene, respectively. Unlike α-pinene has one unsaturated carbon bond, limonene has two unsaturated carbon bond, the nitrate radical can react with either carbon double bond, meanwhile NO and NO_2 formed by nitrate radical can react with alkyl-peroxy radicals (RO_2). Thus, NO will change the formation pathways of SOA and affect the SOA yields (Fry *et al.*, 2014; Liu and Hopke, 2014).

Nitrogen oxides (NO_x) include nitric oxide and nitrogen dioxide. The NO_3 radical is also an important oxidant in indoor chemistry (Nøjgaard, 2010) that can react with some VOCs, such as α-pinene, limonene, and linalool, to produce particles. Indoor NO sources include gas-fired appliances (stoves, ovens, etc.), unvented gas space heaters, unvented kerosene heaters, wood stoves, and environmental tobacco smoke (Brauer *et al.*, 2002; Lee *et al.*, 2002). Indoor fuel combustion has been identified as one of the most significant factors that influence indoor air pollution, especially nitrogen dioxide generation (Lee *et al.*, 2001). NO_2 is produced by oxidation of atmospheric nitrogen during high-temperature fuel combustion. In addition to these major NO_x sources in indoor environments, ventilation/infiltration from outdoors and surface reactions also contribute to indoor NO_x concentrations (Weschler and Shields, 1997; Lee *et al.*, 2002). Since NO_x can cause adverse health effects, including throat irritation, cough, and dyspnea (Samet *et al.*, 1987), indoor NO_x can also represent an important indoor pollutant.

Given the potential importance of the NO oxidation channel and the current paucity of data on such reactions, a study was performed on limonene oxidation in the presence of NO_x. Limonene is one of the most abundant monoterpenes in indoor air. It is widely used in our household products such as a lime-scented (Brauer *et al.*, 2002) liquid air-freshener (Lee *et al.*, 2001), pine-scented solid air-fresher (Weschler and Shields, 1997), lemon-scented, general-purpose cleaner (Singer *et al.*, 2006a) and a perfume (Nojgaard *et al.*, 2006; Sarwar and Corsi, 2007). In this study, the purpose of limonene ozonolysis with NO_x present were investigated to provide new information on SOA yields and the resulting ROS concentrations for different ratios of nitric oxide and ozone similar to the prior study of α-pinene-ozone-NO by Liu and Hopke (2014).

EXPERIMENTAL METHODS

Experimental System Description

Experiments were conducted in a stainless steel chamber (6′ × 4′ × 4′) with an effective volume of 2.5 m^3 and a surface to volume ratio of 4.5 m^{-1} in a temperature controlled room held at 22°C. The chamber was described by Ramamurthi *et al.* (1990) and Hopke *et al.* (1992) and has been used in a number of prior studies of ozone-terpene reaction studies (Chen and Hopke, 2009a, b; 2010; Liu and Hopke, 2014). The environment in the chamber was dark. Fig. 1 shows the schematic diagram of the dynamic chamber set-up. Muffin fans inside the chamber thoroughly mix the air with well-defined turbulence characteristics. Access into the chamber is through a removable face plate fitted with a circular door planted with a septum in the center for added convenience.

Clean air was supplied by drawing compressed air through an air cleaning system that includes a compressed air dryer (Model 3Z528, Dayton Electric MFG Co., Chicago, IL) and a cartridge air filter (Balston, Parker Hannifin Corp., Haverhill, MA) to remove moisture and organic contaminates. An activated charcoal bed was used to remove gaseous organics and ozone. A high-efficiency particulate air (HEPA) filter was used to remove any particles before the air finally reached the mass flow controller (denoted by MFC in Fig. 1) that maintained the flow at the specified flow rate. A pressure transducer with a solenoid valve was used to measure the pressure inside the chamber and to maintain a constant flow of air from the manifold mixer into the chamber.

Ozone-loaded air from a UV ozone generator (UV550, Ozone Solutions Inc., Sioux Center, IA, USA) and nitric oxide (NO) from NO in N_2 gas cylinder were introduced into the chamber and the ozone concentration was monitored by a UV absorption ozone analyzer (49i, Thermo Fisher Scientific Inc, MA) that sampled air at a rate of 1.5 LPM. The NO concentration was measured by a NO_x analyzer (42iTL, Thermo Fisher Scientific Inc, MA) that sampled air at a rate of 1 L min^{-1}. HEPA filters were connected before the ozone and NO_x analyzers to prevent particles in the flow damaging the instruments.

The experiments were conducted at low relative humidity (RH) conditions with the RH below 10%. The low RH prevented any hygroscopic growth of the resulting SOA species and permitted the study of the behavior of the undiluted SOA. Limonene was delivered at an approximately constant concentration from a modified impinger. The flow rates were controlled to provide specific, known VOC concentrations to the chamber. Gaseous samples were collected from the sampling port and analyzed by GC-FID (Trace GC Ultra, Thermo, USA). Gas-tight syringes (A2, VICI Precision sampling Inc. IL, USA) were used to collect hydrocarbon samples. Mixing fans were installed on the ceiling of the chamber to ensure a homogeneous mixing and well-defined turbulence characteristics (Chen and Hopke, 2009a, 2010).

Number and Mass Concentration Measurements

Particle number and size distributions were monitored by a Scanning Mobility Particle Sizer. A TSI model 3071

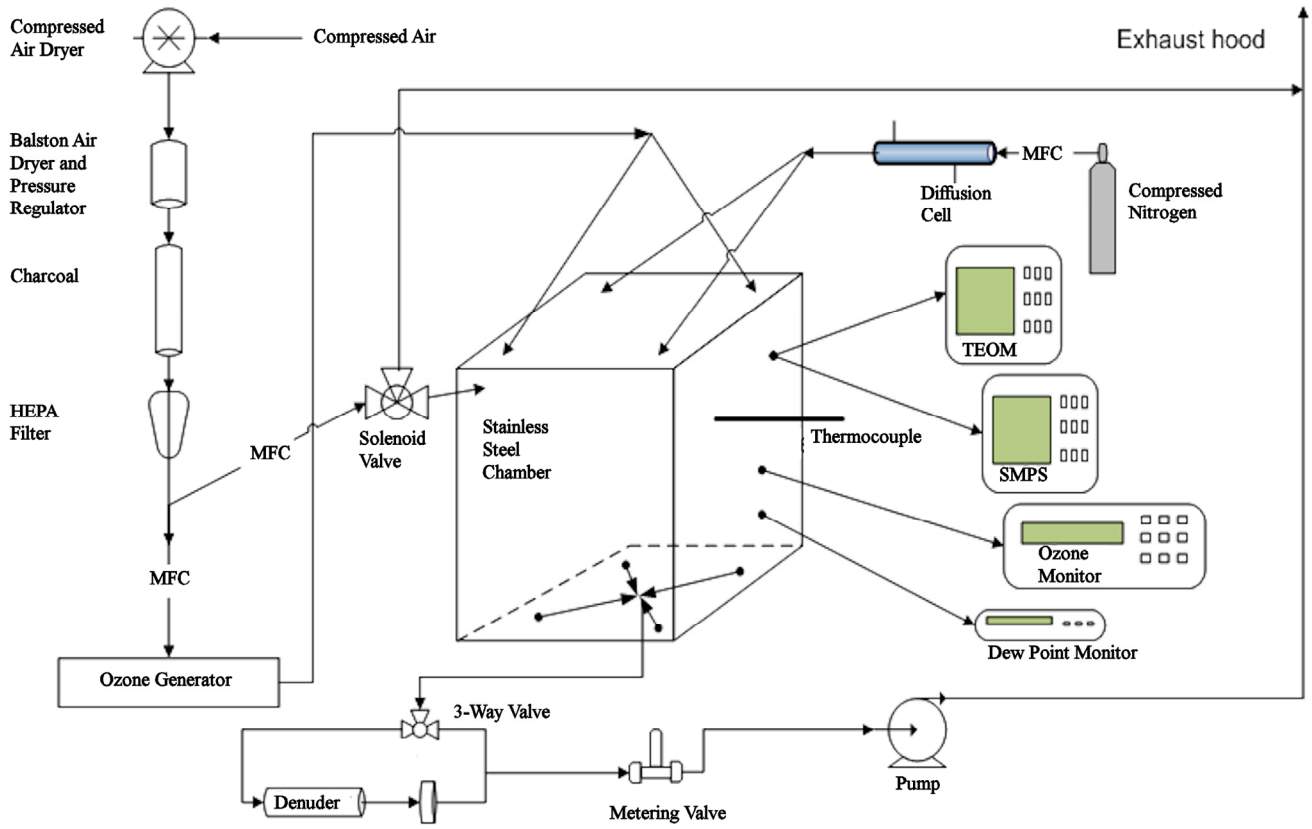

Fig. 1. Schematic diagram of the Clarkson Aerosol Chamber.

DMA coupled with TSI model 3775 Condensation Particle Counter (CPC). The SMPS operated at 3 L min^{-1} and 0.3 L min^{-1} for sheath and aerosol flows, respectively, and measured particle sizes from 14.3 to 680 nm. Size distribution data were recorded and analyzed using TSI AIM v8.1software. The real-time mass concentrations were measured by tapered element oscillation microbalance (TEOM, 1400a, Thermo Fisher Scientific Inc, MA). The TEOM normally operates at an elevated temperature to eliminate the effect of water vapor condensation and to keep the element at a constant temperature. However, heating the sensor causes the loss of semi-volatile species from the particles. Since the experiments were under dry conditions (RH < 10%), elevated temperatures could be avoided to permit measurement of all of the generated SOA mass. Samples for SMPS and TEOM were taken from the middle of the chamber using a metal tube that extended 15 cm through a hole in the face plate. A charcoal denuder was placed before SMPS and TEOM to remove residual gas phase ozone and gas phase organic compounds to prevent further reactions in the collected samples.

Aerosol mass concentrations were sampled on Teflon filters placed inline of outflow on the bottom of the chamber. Filters were weighed in a clean room after collecting samples for 1 hr at flow rate of 23 LPM. These Teflon filters were also used for the ROS measurements. Conductive tubing was used for SMPS, TEOM, and SOA mass collection from the bottom of the chamber and connected to be as short as possible to minimize particle loss to the tubing walls. The wall deposition coefficient was estimated as 0.08 ± 0.01 h^{-1} at an AER of 0.67 ± 0.01 h^{-1} (Chen and Hopke, 2009a). The wall loss correction was used when calculating the overall SOA mass yields.

ROS Measurements

The most effective way to measure ROS is a manual method that uses the reaction of a non-fluorescent probe with oxidants to produce a fluorescent molecule. Aerosol mass concentrations were sampled on Teflon filters placed inline of outflow on the bottom of the chamber. Filters were collected in dark environment and placed in a petri dish covered by aluminum foil before the determination of ROS concentration. The determination of ROS was performed by using a fluorogenic probe, 2',7'—dichlorofluorescin diacetate (DCFH-DA; Calbiochem). Horseradish peroxide (HRP, Sigma Aldrich) was used as the catalyst of the reaction between DCFH and ROS species (Chen and Hopke, 2009b). Fluorescent intensities were converted to equivalent H_2O_2 concentration by using a standard calibration curve. A Turner Quantech Digital Filter Fluorimeter (model # FM109535, Barnstead Thermolyne Corp, Dubuque, IA, USA), with the excitation wavelength set at 485 nm and the emission wavelength set at 525 nm, was employed to monitor the fluorescence intensities.

Samples collected on Teflon filters (Pall, Teflo 25 mm, 3 μm) were extracted immediately by adding the DCFH-HRP working solution and sonicated for 15 min, and then incubated at 37°C for another 15 min. After incubation,

sample solutions were immediately analyzed with the fluorimeter. A few lab blanks were obtained by placing the same Teflon filters in the filter holder and being taken out shortly after (60 to 180 s). These procedures were used consistently to measure resulting fluorescence intensities. The experimental samples were then corrected by subtracting contributions from blank samples.

A linear regression was performed on the experimental data obtained from the measurement of fluorescent intensities of standard H_2O_2 solutions. Fig. 2 shows that the correlation coefficient (R^2 = 0.999) between fluorescent intensity and the H_2O_2 concentration was high. This equation can be used to convert the fluorescent intensity measured for the particle suspension to an equivalent H_2O_2 concentration. This concentration can be interpreted as an indicator of the reactivity of ROS in the particle sample having an oxidizing capability identical to the H_2O_2 solution of the calculated concentration. This concept of equivalent reactivity proposed by Hung and Wang (2001) was used to represent the ROS concentration in particles.

Experimental Procedure

Experiments were conducted with *d*-limonene, ozone, and NO concentrations relevant to indoor concentrations with an effort to keep the VOCs and ozone concentrations approximately constant. NO concentrations were set to almost 0.5, 1, and greater than 2 times the ozone concentrations for the three sets of experiments, respectively. The conditions for each of the experiments are outlined in Table 1. Keeping *d*-limonene concentration constant while varying the NO concentration allows the examination of the effect of the changing ratio of ozone and NO with regards to the particle number concentrations and SOA mass produced. Experiments were conducted at room temperature (22°C) and an air exchange rate of 0.67 ± 0.01 h^{-1}. Prior to an experiment, the chamber is flushed with purified air for 24 h to remove the particles, VOCs, and any residue from the prior experiment. Then the chamber was flushed with the compressed air. The resultant background particle concentration was less than 100 particles cm^{-3}, mass concentrations less than 0.2 μg m^{-3} and negligible NO_x with concentrations lower than 3 ppb. Ozone and NO were first continuously introduced into chamber and several hours were allowed for the concentrations inside the chamber to reach steady state. Then the *d*-limonene was added to the chamber from the diffusion cell at a constant concentration and flow rate.

The experiments were conducted under low relative humidity (RH) conditions that could be regarded as dry with

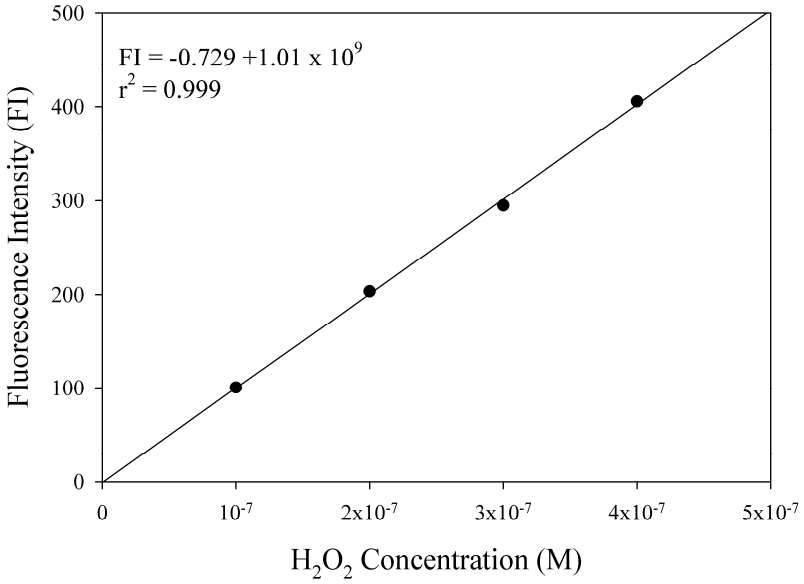

Fig. 2. Fluorescence intensity of DCF obtained by reaction of DCFH with H_2O_2 solutions of indicated concentrations.

Table 1. Experimental conditions for different ratios of reagents.

date	Initial limonene (ppb)	Initial ozone (ppb)	Initial NO_x (ppb)	Initial NO_x/O_3	Limonene s.s* (ppb)	Ozone s.s (ppb)	NO_x s.s (ppb)	AER (h^{-1})	T (°C)	RH (%)
3/10/2013	154	69.7	33.7	0.48	108.2	45.7	1176	0.67 ± 0.01	22–23	9.6–9.9
3/17/2013	150	71.0	35.2	0.50	102	46.5	1179	0.67 ± 0.01	22–23	9.4–9.6
3/25/2013	158	72.1	58.9	0.82	118.7	1167	415	0.67 ± 0.01	22–24	9.5–9.8
3/31/2013	153	70.3	62.4	0.89	112.3	1158	411	0.67 ± 0.01	23–24	9.4–9.6
4/5/2013	155	1.1	67.1	61.0	129.3	0.8	1227	0.67 ± 0.01	23–24	9.7–9.9
4/14/2013	159	0.9	68.2	75.9	134.3	1	1196	0.67 ± 0.01	22–23	9.2–9.6

s.s* = steady state.

the RH around 9–10%. This condition was chosen to prevent the hygroscopic growth of the resulting SOA species and permit the study of behavior of the undiluted SOA.

RESULT AND DISCUSSION

Concentration Ratio of NO/O_3 Approximately around 0.83

The ozone and NO_x concentrations were monitored continuously. For this set of conditions, NO was consumed, NO_2 increased continuously and remained constant after reaching steady state. Since the ozone concentrations were somewhat above those of the NO because of the inability to control them precisely, there was untitrated ozone in the chamber. At this point, the known concentration of *d*-limonene was introduced into the chamber by the carrier gas N_2. Fig. 3 shows the typical evolution of the SOA concentration as well as ozone and NO_x concentrations beginning at the point when the limonene was introduced to the chamber with steady-state condition for ozone and NO_x. This point is defined as the time zero point in the figure. The sum of particle sizes from 14.6 to 661 nm was used to calculate the total number concentration. With the AER at 0.67 ± 0.01 h^{-1}, it took around 3h for the number and total mass to arrive the steady-state concentration after adding the *d*-limonene as seen in Fig. 3.

The trend of the particle number concentration can be divided into three stages. After introducing the *d*-limonene into the chamber, there was a sudden burst of small particles. The total number concentration increased and then decreased but with a shift in size to larger particles. As the larger particles were produced in the chamber, the number concentration started to decline. The number concentration continued to decrease while the mass concentration kept increasing. Around 3 hours (vertical solid line), both the number and mass concentrations approached steady-state with the values of 8×10^4 # cm^{-3} and 170 μg m^{-3}. At just over 8 hours (vertical dashed line), the reactive species were turned off and the concentrations declined with the continued ventilation with clean air.

The NO concentration followed a similar pattern to the mass concentration, and was about 414 ppb at steady state. However, the ozone concentration kept increasing until 5.5 h and then reached the steady state at 1167 ppb. Because of the rapid reaction between ozone and NO (rate constant = 1.81×10^{-14} cm^3 $molecule^{-1}$ s^{-1}), the concentration of NO remained low over the whole experiment. The *d*-limonene will not react with NO_2. Thus, to understand the particle formation observed, either the *d*-limonene only reacts with a small portion of fresh ozone that is continuously introduced into the chamber before it can react with NO or there may be a slight imbalance between the NO and O_3 concentrations given the limitations on flow control and concentration measurements.

Concentration Ratio of NO/O_3 Equal to 0.5

The second set of experiments was conducted at a concentration ratio of NO/O_3 approximately 0.5. The flow rate of O_3 was approximately twice that of the NO provided. The additional O_3 can react with the NO_2 generated from the reaction between NO and O_3 to nitrate radical (NO_3) (Pandis and Seinfeld, 2006). The results of the experiment on 3/10/2013 are shown in Supplemental Fig. S1. Although particle concentration data were collected and the results presented in Table 2, the SMPS values have been lost in the intervening period and are not presented. In this case, there is oxidation of the limonene by the nitrate radical resulting in the highest concentrations of particles, SOA, and ROS. This pattern is similar that observed by Liu and Hopke (2014) in comparable experiments with α-pinene.

Concentration Ratio of NO/O_3 Greater than 2

For the third set of experiments, the flow rate of NO was

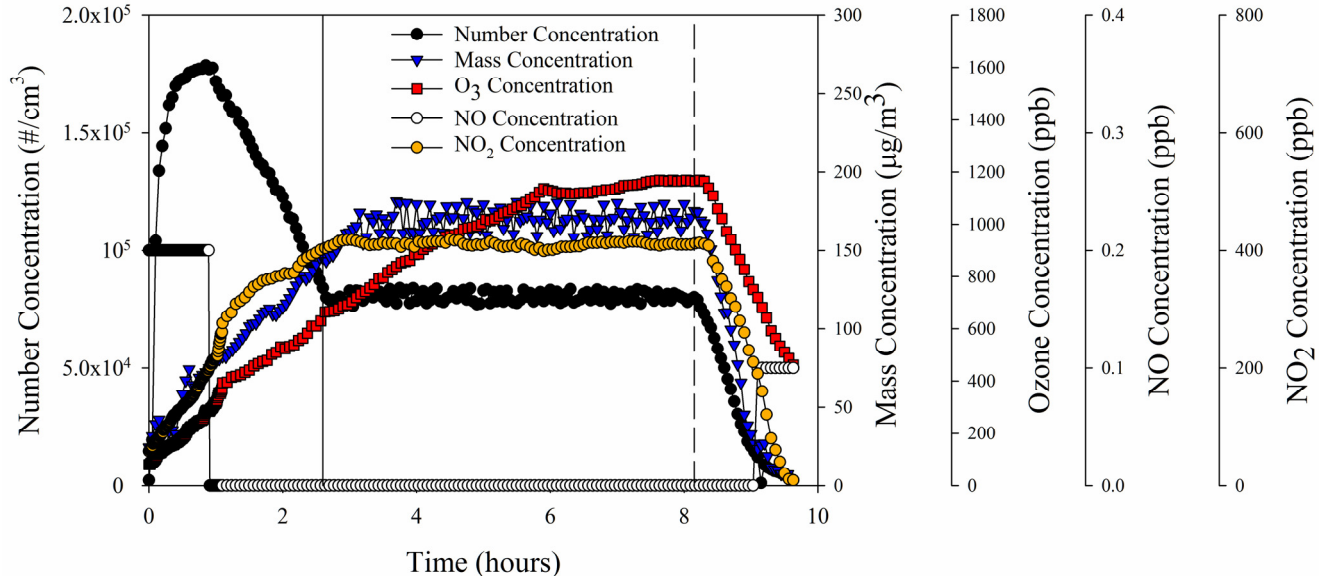

Fig. 3. Time series of number, mass, ozone, nitric oxide and nitrogen oxides concentration for experiment 3/25/2013; limonene, nitric oxide and ozone supply stopped at around 8 h after the introduction of limonene to the chamber.

Table 2. Experiment results.

date	Initial limonene (ppb)	Initial ozone (ppb)	Initial NO_x (ppb)	Initial NO_x/O_3	s.s. *d*-limonene (μg m^{-3})	ss SOA mass conc. (μg m^{-3})	Yield	Density (g cm^{-3})	s.s. ROS (nmol m^{-3})	Particle formation rate (# cm^{-3} h^{-1})
3/10/2013	154	69.7	33.7	0.48	257	135.7	0.49	1.36	22.08	39108
3/17/2013	150	71.0	35.2	0.50	269	137.2	0.51	1.37	21.97	38044
3/25/2013	158	72.1	58.9	0.82	220	156.5	0.73	1.22	28.32	58902
3/31/2013	153	70.3	62.4	0.89	228	157.3	0.72	1.21	29.44	57412
4/5/2013	155	1.1	67.1	61.0	144	30.3	0.27	1.47	6.12	467
4/14/2013	159	0.9	68.2	75.9	138	31.8	0.30	1.48	7.26	455

set to be much greater that of O_3. The actual ozone concentrations were very low due to a leak from the ozone generator into the room. Under these conditions, O_3 was totally consumed by NO to form NO_2, Neither NO and NO_2 can react with *d*-limonene, and thus few particles and little PM mass and ROS were formed in the chamber. The results of the experiment on April 5, 2013 are shown in Supplemental Fig. S2. Thus, in a home with high NO emissions from a gas stove, small amounts of infiltrated ozone will not have any effect on indoor particle formation with available reactive hydrocarbon compounds.

SOA Yields and Densities

Six sets of experiments were conducted at different precursor concentration ratios resulting in different steady state SOA mass concentrations. Keeping a constant *d*-limonene concentration while varying the flows of NO and O_3 helped to evaluate the effect of changing the reagents with the number concentrations and SOA mass produced. Given that the reactions among limonene, ozone, and NO are second-order reaction, the SOA formation should be proportional to initial concentrations of the reagents. Samples, collected for 1 h at a flow rate of 23 L min^{-1} on pre-weighed Teflon filters (Pall, Teflo 25 mm, 3 μm) at the bottom of the chamber, were used to measure the SOA mass concentration after the system reached steady state. The filters were weighed again after sampling in a clean room with controlled temperature (23°C, 35% RH).

Secondary organic aerosol formation can be determined experimentally through investigation of the fractional aerosol yield, Y (Pandis *et al.*, 1991; Zhang *et al.*, 1992). The approach developed by Odum *et al.* (1996) related the SOA yield defined as the mass of SOA formed per mass of hydrocarbon consumed with the SOA mass concentration.

$$Y=\frac{\Delta M}{\Delta HC}=M\sum\frac{\alpha_i K_{p,i}}{1+MK_{p,i}} \quad (1)$$

where Y is the resulting yield, ΔM and M refer to the organic aerosol mass concentration (μg m^{-3}), ΔHC is the consumed hydrocarbon concentration (μg m^{-3}), and $K_{p,i}$ and α_i are the partitioning coefficient and mass yield of compound i, respectively. This model has been successfully used to calculate the yield data for many experiments (Presto and Donahue, 2006; Chen and Hopke, 2009a; b, 2010; Liu and Hopke, 2014).

According to the organic mass concentration and consumed hydrocarbon concentration, Eq. (1) was used to calculate the SOA yield for the sum of the semi-volatile species produced. This method has been found to successfully fit the yield result in many studies (Odum *et al.*, 1996; Nojgaard *et al.*, 2006; Chen and Hopke, 2009a, b). Table 2 shows that the ratio of NO_x/O_3 around 0.83 produced the highest yield (0.73) in all of the experiments. The yield has almost three times than the value of NO_x/O_3 ratio > 2. The result shows that little SOA was produced in the low O_3 concentration, due to the fact that there was not sufficient O_3 to fully oxidize the parent compound. Thus, high indoor NO concentrations would suppress the formation of SOA and ROS although it represents its own health threats (Samet *et al.*, 1987).

By comparing the mass concentrations with the volume concentrations calculated from the number size distributions, the densities of SOA were estimated and are shown in Table 2. The change in density with the corresponding SOA mass concentrations showed a decrease in density as the SOA mass loading increased (Fig. 4). The trend was found to be opposite to that of the yield data, the ratio of NO_x/O_3 > 2 has the highest SOA density about 1.47 g cm^{-3}, while the ratio NO_x/O_3 around 0.83 has the smallest density about 1.21 g cm^{-3}. The correlation coefficient (r^2) of SOA mass concentration and density is 0.8. The decreasing density with increasing SOA mass is similar to what was observed for limonene and ozone without NO present (Chen and Hopke, 2010). It is attributed to increased absorption of the unreacted limonene into the SOA droplets. The unreacted limonene will have a lower density than the more oxygenated SOA species and thus, increasing the limonene concentration in the SOA particle will reduce its density.

Calculation of Particle Formation Rates

Upon the chamber reaching the steady state, the number concentration remained constant, the particle balance in the system is given by

$$V\frac{dC_N}{dt}=FR\times V-AER\times C_N\times V-k_{wall}\times C_N\times V \quad (2)$$

where V is the volume of the chamber (m^3), AER is the air exchange rate (h^{-1}), C_N is the particle number concentration (# cm^{-3}), k_{wall} is the particle wall loss deposition coefficient

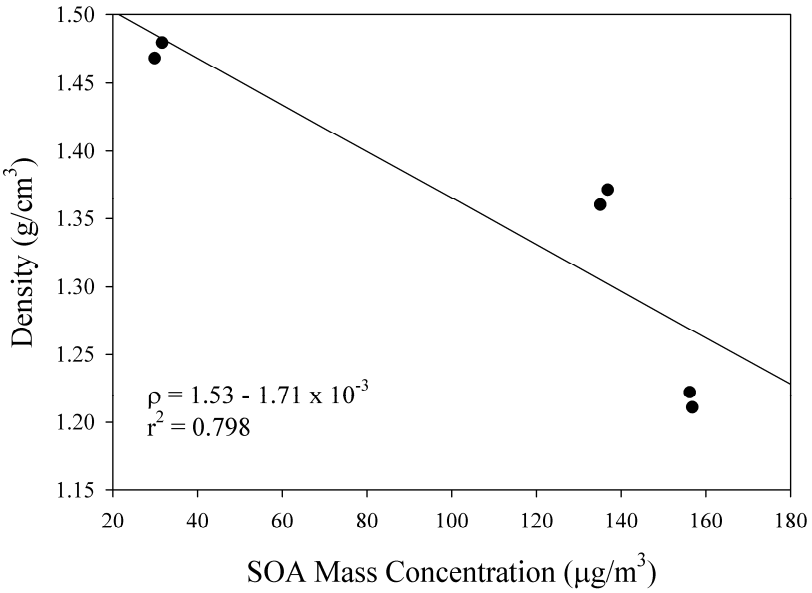

Fig. 4. Densities of SOA produced VS SOA mass concentration at steady state ($R^2 = 0.80$).

(h^{-1}), FR is the particle formation rate (# h^{-1}). When the steady state, $dC_N/dt = 0$, was obtained, the particle formation rate can be estimated according to the loss from dilution by air exchange and chamber wall loss. The calculated particle formation rates are shown in Table 2. The range was from 455 to 5.89×10^4 # cm^{-3} h^{-1} and the highest particle formation rate was found at the ratio of initial NO_x/O_3 concentration of about 1.2, and the highest particle formation rate was 100 times more than those produced by the ratio of initial NO_x/O_3 concentration greater than 2. The results were 10 times than the limonene-ozone system (Chen and Hopke, 2010). As shown in Fig. 5, the change of initial reagents (limonene × O_3 × NO) concentration (ppb^3) determined the trend of both SOA mass and particle formation rate. The highest initial reagent concentrations resulted in the highest formation rate with 5.89×10^4 # cm^{-3} h^{-1}. However, the rate of increase slowed at higher reagent concentrations, which means under the conditions of constant AER and at higher mass production, condensable material preferred to condense onto the existing particles rather than nucleating to produce additional new particles (McMurry and Friedlander, 1979).

ROS Concentrations

Reactive oxygen species (ROS) contains a variety of species including free radicals such as OH, HO_2 and organic peroxy radicals that include molecules like H_2O_2 and organic peroxides as well as ions like superoxide anion (Weschler and Shields, 1996; Venkatachari and Hopke, 2008). Docherty *et al.* (2005) investigated the contribution of organic peroxides to SOA which was produced from α-pinene and β-pinene oxidation and accounted for 47% and 85% of all generated SOA. Both gas-phase and particle-bound ROS can be produced by the chemical reaction. Because particle-bound ROS can more effectively penetrate into human lungs than gas phase ROS, it may cause more adverse health problems than gas-phase ROS.

Samples for ROS measurement were collected over 1 hour intervals after the system reached steady state using a flow rate of 23 LPM. Similar to the previous studies (Chen and Hopke, 2009b, 2010), the particle-bound SOA concentration decreases over time because the short-lived free radical species such as OH, RO, HO_2 and RO_2 decompose and re-equilibrium of the collected volatile compounds is established. Those results suggest the importance of immediately extracting and measuring of the SOA samples. The determined ROS concentrations of the different experiment are shown in Table 2.

The ROS concentrations ranged from 6.1 to 29.4 nmol m^{-3} equivalents of H_2O_2. The highest ROS concentration, found for the ratio of initial NO/O_3 around 1, was 29.4 nmol m^{-3}, while the lowest data was found in the ratio of initial NO/O_3 around 700, was 6.1 nmol m^{-3}. The development of SOA showed similar patterns of yield and concentration as shown in Fig. 6. The highest SOA mass concentration had the highest ROS concentration and yield, while the lowest SOA mass has the lowest ROS concentration and lowest yield (Table 2). The higher SOA with higher ROS is expected to include more oxygenated species (e.g., organic peroxides). Up to one order of magnitude higher ROS concentrations were observed relative to those observed in ambient air in Rubidoux, CA, an urban site in the eastern Los Angeles basis with substantial photochemical activity. Thus, if oxidative stress is a cause of the adverse health effects observed to result from exposure to ambient particulate matter, then these more oxidizing indoor particles could certainly induce similar effects (Weschler, 2006).

The concentrations in these experiments were higher than previous chamber studies. Under the same conditions of initial reagents concentration (ppb^2), limonene ozonolysis produced the more ROS than in linalool or α-pinene ozonolysis. Given the complexity of ROS constituents and the reaction between monoterpenes and ozone in the presence of NO_x, further studies should be taken to identify the nature of ROS species.

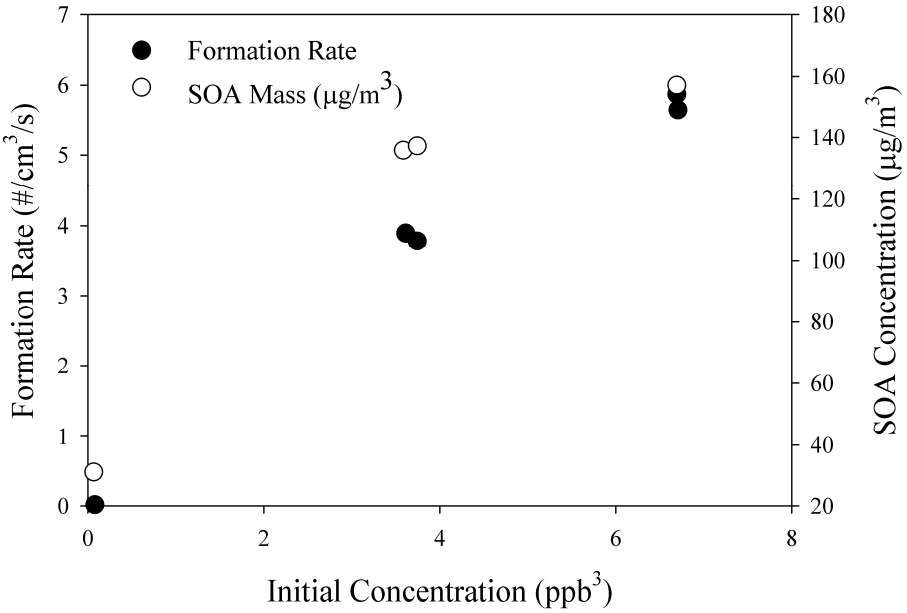

Fig. 5. Particle number formation rate and SOA mass as a function of product of initial ozone, NO and limonene concentrations.

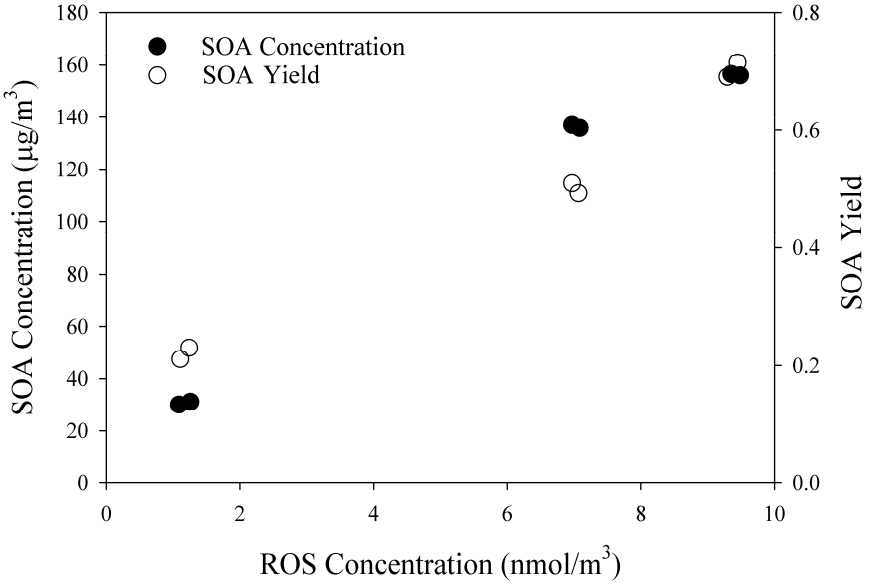

Fig. 6. SOA mass and yield as a function of ROS concentration.

CONCLUSIONS

The experiments on limonene ozonolysis in the presence of NO in a flow chamber system simulate reactions that might be expected to occur in indoor air between infiltrated ozone and limonene off-gassed from household products. The characteristics of the resulting SOA and ROS for initial reagents concentration relevant to the indoor environment were investigated and quantified. The yield of SOA resulting from the reaction between limonene and ozone was higher than α-pinene and linalool studies. ROS concentration was also higher than two other chamber studies. Thus, the risk of human health from the exposure to high ROS and SOA cannot be ignored (Weschler, 2006).

Results from this study show that SOA in higher quantity will result from events when the initial NO_x/O_3 ratio was around 1. High SOA mass produced is accompanied by high ROS concentration. Thus, the particle formation rate was consistent with the pattern of SOA mass. Appliances that produce NO_x should always be vented to the outside of the house (lee *et al.*, 1998). It is difficult to control ozone concentration coming from outdoors, but exposure to SOA and ROS can be minimized by changing to household products that do not contain ozone-reactive constitutes. Product substitution will be the most effective way to control indoor SOA formation.

ACKNOWLEDGMENT

This work was supported by the Natural Science Foundation of Jiangsu Province, China (BK20160102), and the Central Research Institutes of Basic Research and Public Service special operations (20160302). The authors are grateful to CARES at Clarkson University for the convenience of the study. The authors also appreciate the help from Dr. Hongxia Yu of Nanjing University of Science and Technology.

SUPPLEMENTARY MATERIAL

Supplementary data associated with this article can be found in the online version at http://www.aaqr.org.

REFERENCES

Brauer, M., Hoek, G., Van Vliet, P., Meliefste, K., Fischer, P.H., Wijga, A., Koopman, L.P., Neijens, H.J., Gerritsen, J., Kerkhof, M., Heinrich, J., Bellander, T. and Brunekreef, B. (2002). Air pollution from traffic and the development of respiratory infections and asthmatic and allergic symptoms in children. *Am. J. Respir. Crit. Care Med.* 166: 1092–1098.

Carslaw, N., Mota, T., Jenkin, M.E. and Barley, M.H. (2012). A significant role for nitrate and peroxide groups on indoor secondary organic aerosol. *Environ. Sci. Technol.* 46: 9290–9298.

Chen, X. and Hopke, P.K. (2009a). A chamber study of secondary organic aerosol formation by linalool ozonolysis. *Atmos. Environ.* 43: 3935–3940.

Chen, X. and Hopke, P.K. (2009b). Secondary organic aerosol from α-pinene ozonolysis in dynamic chamber system. *Indoor Air* 19: 335–345.

Chen, X. and Hopke, P.K. (2010). A chamber study of secondary organic aerosol formation by limonene ozonolysis. *Indoor Air* 20: 320–328.

Destaillats, H., Maddalena, R.L., Singer, B.C., Hodgson, A.T. and McKone, T.E. (2008). Indoor pollutants emitted by office equipment: A review of reported data and information needs. *Atmos. Environ.* 42: 1371−1388.

Docherty, K.S., Wu, W., Lim, Y.B. and Ziemann, P.J. (2005). Contributions of organic peroxides to secondary aerosol formed from reactions of monoterpenes with O_3. *Environ. Sci. Technol.* 39: 4049–4059.

Du, X. and Liu, J. (2009). Relationship between outdoor and indoor ozone pollution concentration. *Trans. Tianjin Univ.* 15: 330–335.

Fry, J.L., Draper, D.C., Barsanti, K.C., Smith, J.N., Ortega, J., Winkler, P.M., Lawler, M.J., Brown, S.S., Edwards, P.M., Cohen, R.C. and Lee, L. (2014). Secondary organic aerosol formation and organic nitrate yield from NO_3 oxidation of biogenic hydrocarbons. *Environ. Sci. Technol.* 48: 11944–11953.

Guenther, A., Geron, C., Pierce, T., Lamb, B., Harley, P. and and Fall, R. (2000). Natural emissions of non-methane volatile organic compounds, carbon monoxide, and oxides of nitrogen from North America. *Atmos. Environ.* 34: 2205–2230.

Hatfield, M.L. and Hartz, K.E.H. (2011). Secondary organic aerosol from biogenic volatile organic compound mixtures. *Atmos. Environ.* 45: 2211–2219.

HHS/NIH (2015). Household Products Database: *D*-limonene. National Library of Medicine. National Institute of Health. http://householdproducts.nlm.nih.gov/cgi-bin/household/brands?tbl=chemid=166.

Hopke, P.K., Ramamurthi, M., Knutson, E.O., Tu, K.W., Scofield, P., Holub, R.F., Cheng, Y.S., Su, Y.F., Winklmayr, W., Strong, J.C., Solomon, S. and Reineking, A. (1992). The measurement of activity-weighted size distributions of radon progeny: Methods and laboratory intercomparison studies. *Health Phys.* 63: 560–570.

Hung, H.F. and Wang, C.S. (2001). Experimental determination of reactive oxygen species in Taipei aerosols. *J. Aerosol Sci.* 32: 1201–1211.

Kamens, R., Jang, M., Chien, C.J. and Leach, K. (1999). Aerosol formation from the reaction of α-pinene and ozone using a gas-phase kinetics-aerosol partitioning model. *Environ. Sci. Technol.* 33: 1430–1438.

Lee, B.H., Pierce, J.R., Engelhart, G.J. and Pandis, S.N. (2011). Volatility of secondary organic aerosol from the ozonolysis of monoterpenes. *Atmos. Environ.* 45: 2443–2452.

Lee, K., Levy, J.I., Yanagisawa, Y., Spengler, J.D. and Billick, I.H. (1998). The Boston residential nitrogen dioxide characterization study: Classification and prediction of indoor NO_2 exposure. *J. Air Waste Manage. Assoc.* 48: 736–742.

Lee, K., Xue, J., Geyh, A.S., Ozkaynak, H., Leaderer, B.P., Weschler, C.J. and Spengler, J.D. (2002). Nitrous acid, nitrogen dioxide, and ozone concentrations in residential environments. *Environ. Health Perspect.* 110: 145–149.

Lee, S.C., Lam, S. and Ho, K.F. (2001). Characterization of VOCs, ozone, and PM_{10} emissions from office equipment in an environmental chamber. *Build. Environ.* 36: 837–842.

Leungsakul, S., Jaoui, M. and Kamens, R.M. (2005). Kinetic mechanism for predicting secondary organic aerosol formation from the reaction of *d*-limonene with ozone. *Environ. Sci. Technol.* 39: 9583–9594.

Li, T.H., Turpin, B.J., Shields, H.C. and Weschler, C.J. (2002). Indoor hydrogen peroxide derived from ozone/*d*-limonene reactions. *Environ. Sci. Technol.* 36: 3295–3302.

Liu, Y. and Hopke, P.K. (2014). A chamber study of secondary organic aerosol formed by ozonolysis of α-pinene in the presence of nitric oxide. *J. Atmos. Chem.* 71: 21–32.

McMurry, P.H. and Friedlander, S.K. (1979). New particle formation in the presence of an aerosol. *Atmos. Environ.* 13: 1635–1651.

Morawska, L., He, C.R., Johnson, G., Guo, H., Uhde, E. and Ayoko, G. (2009). Ultrafine particles in indoor air of a school: Possible role of secondary organic aerosols. *Environ. Sci. Technol.* 43: 9103−9109.

Nojgaard, J.K., Bilde, M., Stenby, C., Nielsen, O.J. and Wolkoff, P. (2006). The effect of nitrogen dioxide on particle formation during ozonolysis of two abundant

monoterpenes indoors. *Atmos. Environ.* 40: 1030–1042.
Nøjgaard, J.K. (2010). Indoor measurements of the sum of the nitrate radical, NO_3, and nitrogen pentoxide, N_2O_5 in Denmark. *Chemosphere* 79: 898–904.
Odum, J.R., Hoffmann, T., Bowman, F., Collins, D., Flagan, R.C. and Seinfeld, J.H. (1996). Gas/particle partitioning and secondary organic aerosol yields. *Environ. Sci. Technol.* 30: 2580–2585.
Pandis, S.N., Paulson, S.E., Seinfeld, J.H. and Flagan, R.C. (1991). Aerosol formation in the photooxidation of isoprene and α-pinene. *Atmos. Environ.* 25: 997–1008.
Pavlovic, J. and Hopke, P.K. (2011). Detection of radical species formed by the ozonolysis of α-pinene. *J. Atmos. Chem.* 66: 137–155.
Presto, A.A., Huff Hartz, K.E. and Donahue, N.M. (2005). Secondary organic aerosol production from terpene ozonolysis. 2. Effect of NO_x concentration. *Environ. Sci. Technol.* 39: 7046–7054.
Presto, A.A. and Donahue, N.M. (2006). Investigation of α-pinene + ozone secondary organic aerosol formation at low total aerosol mass. *Environ. Sci. Technol.* 40: 3536–3543.
Ramamurthi, M., Strydom, R. and Hopke, P.K. (1990). Assessment of wire and tube penetration theories using a 218PoOx cluster aerosol. *J. Aerosol Sci.* 21: 203–211
Samet, J.M., Marbury, M.C. and Spengler, J.D. (1987). Respiratory effects of indoor air pollution. *J. Allergy Clin. Immunol.* 79: 685–700.
Santiago, M., Vivanco, M.G. and Stein, A.F. (2012). Evaluation of CMAQ parameterizations for SOA formation from the photooxidation of alpha-pinene and limonene against smog chamber data. *Atmos. Environ.* 56: 236–245.
Sarwar, G. and Corsi, R. (2007). The effects of ozone/limonene reactions on indoor secondary organic aerosols. *Atmos. Environ.* 41: 959–973.
Seinfeld, J.H. and Pandis, S.N. (2006). *Atmospheric Chemistry and Physics: From Air Pollution to Climate Change*, 2nd Edition, J. Wiley & Sons, Inc., New York, pp. 1232.
Singer, B.C., Destaillats, H., Hodgson, A.T. and Nazaroff, W.W. (2006a). Cleaning products and air fresheners: emissions and resulting concentrations of glycol ethers and terpenoids. *Indoor Air* 16: 179–191.
Singer, B.C., Coleman, B.K., Destaillats, H., Hodgson, A.T., Lunden, M.M., Weschler, C.J. and Nazaroff, W.W. (2006b). Indoor secondary pollutants from cleaning product and air freshener use in the presence of ozone. *Atmos. Environ.* 40: 6696–6710.
Spittler, M., Barnes, I., Bejan, I., Brockmann, K.J., Benter, T. and Wirtz, K. (2006). Reactions of NO_3 radicals with limonene and α-pinene: Product and SOA formation. *Atmos. Environ.* 40: 116–127.
Venkatachari, P., Hopke, P.K., Brune, W.H., Ren, X., Lesher, R., Mao, J. and Mitchell, M. (2007). Characterization of wintertime reactive oxygen species concentrations in flushing, New York. *Aerosol Sci. Technol.* 41: 97–111.
Venkatachari, P. and Hopke, P.K. (2008). Characterization of products formed in the reaction of ozone with α-pinene: Case for organic peroxides. *J. Environ. Monit.* 10: 966–974.
Waring, M.S., Wells, J.R. and Siegel, J.A. (2011). Secondary organic aerosol formation from ozone reactions with single terpenoids and terpenoid mixtures. *Atmos. Environ.* 45: 4235–4242.
Weschler, C.J., Shields, H.C. and Naik, D.V. (1989). Indoor ozone exposures. *J. Air Pollut. Control Assoc.* 39: 1562–1568.
Weschler, C.J. and Shields, H.C. (1996). Production of hydroxyl radicals in indoor air. *Environ. Sci. Technol.* 30: 3250–3258
Weschler, C.J. and Shields, H.C. (1997). Potential reactions among indoor pollutants. *Atmos. Environ.* 31: 3487–3495.
Weschler, C.J. and Shields, H.C. (1999). Indoor ozone/terpene reactions as a source of indoor particles. *Atmos. Environ.* 33: 2301–2312.
Weschler, C.J. (2000). Ozone in indoor environments: Concentration and chemistry. *Indoor Air* 10: 269–288.
Weschler, C.J. (2004). Chemical reactions among indoor pollutants: What we've learned in the new millennium. *Indoor Air* 14: 184–194.
Weschler, C.J. (2006). Ozone's impact on public health: contributions from indoor exposures to ozone and products of ozone-initiated chemistry. *Environ. Health Perspect.* 114: 1489–1496.
Youssefi, S. and Waring, M.S. (2012). Predicting secondary organic aerosol formation from terpenoid ozonolysis with varying yields in indoor environments. *Indoor Air* 22: 415–426.
Zhang, J.Y., Hartz, K.E.H., Pandis, S.N. and Donahue, N.M. (2006). Secondary organic aerosol formation from limonene ozonolysis: Homogeneous and heterogeneous influences as a function of NO_x. *J. Phys. Chem. A* 110: 11053–11063.
Zhang, S.H., Shaw, M., Seinfeld, J.H. and Flagan, R.C. (1992). Photochemical aerosol formation from α-pinene- and β-pinene. *J. Geophys. Res.* 97: 20717–20729.

Received for review, January 19, 2016
Revised, July 18, 2016
Accepted, July 20, 2016